Acoustic band gaps in fibre composite materials of boron nitride structure

1997 J. Phys.: Condens. Matter 9 7327

(http://iopscience.iop.org/0953-8984/9/35/008)

J. Phys.: Condens. Matter **9** (1997) 7327–7341. Printed in the UK PII: S0953-8984(97)84165-3

Acoustic band gaps in fibre composite materials of boron nitride structure

J O Vasseur†, B Djafari-Rouhani†, L Dobrzynski† and P A Deymier‡

† Equipe de Dynamique des Interfaces, Laboratoire de Dynamique et Structures des Matériaux Moléculaires, URA CNRS No 801, UFR de Physique, Université de Lille I, 59655 Villeneuve d'Ascq Cédex, France

‡ Department of Materials Science and Engineering, University of Arizona, Tucson, AZ 85721, USA

Received 14 May 1997

Abstract. We present elastic band-structure results for a new geometry of two-dimensional phononic crystals: the boron nitride- (BN-) like structure. This array is constituted of two kinds of infinite elastic parallel cylinder located at the vertices of a regular hexagon and surrounded by an elastic background. This geometry includes both the triangular and graphite structures as particular cases. The inclusions and matrix are either both fluids or both solids, the constituent materials being water and mercury, and carbon (or tungsten) and epoxy.

We discuss the evolution of the band structure, and especially the existence of absolute band gaps, as a function of the ratio between the radii of the two cylinders in the BN geometry. We also discuss the existence of these gaps in relation to the physical parameters of the materials involved, and compare the results with those for square and triangular structures.

1. Introduction

During the last ten years, the propagation of electromagnetic waves in binary periodic artificial structures called 'photonic crystals' has received a great deal of attention. These inhomogeneous materials constituted of dielectric inclusions embedded in a dielectric matrix may present original physical properties such as the existence of forbidden bands in their electromagnetic band structures. These gaps could lead to inhibited spontaneous emission as well as to the localization of photons [1].

The analogy between electromagnetic waves and vibrations stimulated research on the propagation of acoustic waves in 'phononic crystals' constituted of elastic inclusions surrounded by an elastic medium [2]. Acoustic gaps being frequency domains in which propagation of sound and phonons are forbidden, one can imagine for these phononic crystals numerous engineering applications such as vibrationless environments for high-precision mechanical systems, or the design of transducers. Various structures of phononic crystals were studied. The existence of large gaps in the acoustic band structures of cubic lattices of elastic spherical inclusions surrounded by a host matrix has been established, the constituent materials being either both solids [3, 4] or both fluids [5, 6]. Complete acoustic band gaps were also obtained in two-dimensional phononic crystals constituted of periodic arrays of elastic solid (or fluid) rods embedded in an elastic solid (or fluid) background.

0953-8984/97/357327+15$19.50

Square [4, 7–10] and triangular [4, 11–13] lattices were investigated. The propagation of elastic waves in one-dimensional systems such as superlattices [14–17] has also been studied extensively during the last few decades.

In all of these composite systems, the contrast in elastic properties and densities between the constituents, and the composition of the inhomogeneous artificial material are emerging as critical parameters in determining the existence of acoustic gaps [2].

In this paper, we present results on the elastic band structure for a new geometry of two-dimensional phononic crystals: the boron nitride- (BN-) like structure, in which the infinite circular elastic rods are located at the vertices of a regular hexagon and are surrounded by an elastic background. The unit cell of the Bravais lattice contains two kinds of infinitely long parallel cylinder [18, 19]. With two cylinders of identical radius, constituted of the same material, the graphite structure is obtained, while if the radius of one of the two cylinders is infinitely small, the already widely studied triangular structure [4, 11–13] is generated. We define the triangular structure, in accordance with the terminology used by Plihal and Maradudin [20], as the 2D array in which the cylinders are located at the vertices and at the centre of a regular hexagon. This pattern is often called 'hexagonal structure' in the literature [4, 11–13]. In the BN structure, in addition to the contrast in densities and elastic parameters, the ratio $\alpha = R_1/R_2$ between the radii of the cylinders appears as a pertinent parameter in determining the existence of acoustic band gaps. The analogy between electromagnetic waves and vibrations, and recent results on photonic crystals showing the existence of large absolute band gaps for the triangular structure of cylindrical holes in a dielectric background and for graphite structure of dielectric rods in air [18, 19] have motivated this study.

We consider, in this paper, 2D composite media, for which the inclusions and the matrix are either both fluids or both solids, cylindrical inclusions being disposed on BN arrays. The physical realization of a 2D fluid/fluid composite system could be achieved by inserting the inclusion material in a latex bladder. The dispersion curves are computed for water (or mercury) cylinders in a mercury (or water) background, and for carbon or tungsten (or epoxy) circular rods in an epoxy (or C or W) matrix. These band structures will be discussed as a function of the parameter α, for different values of the inclusions filling fraction f. For the practical realization of large acoustic band gaps, the graphite structure, and more generally the BN geometry, can appear as better than, similar to, or worse than the most-studied triangular structure, depending on the values of α and f and on the material parameters. For example, in the fluid composites, the graphite structure is more favourable for mercury cylinders in a water background, both for high and low filling fractions. In the opposite case of water rods in mercury, the triangular structure gives rise to the largest band gap, but the BN and graphite geometries may allow several additional gaps of similar magnitude. In the case of solid composites, the coexistence of three different polarizations makes the formation of absolute acoustic band gaps more difficult. The graphite and some BN patterns will be more interesting than the triangular structure, for instance, for a low filling fraction of W fibres in epoxy or a high filling fraction of epoxy fibres in C or W. We show that selective noise filters could be obtained from BN arrays of cylindrical inclusions of very different radii. In this work, we shall also compare our results for the triangular structure to those of the previous studies of both triangular and square lattices.

The paper is organized as follows. The model and the method of calculation are briefly presented for fluid/fluid and solid/solid binary 2D composite media in section 2. We discuss the numerical results in section 3, and draw conclusions in section 4.

2. The model and method of calculation

2.1. The model

In this paper, we calculate elastic band structures for solid/solid and fluid/fluid 2D binary composite systems using a method developed by Kushwaha *et al* [8–10, 13]. These periodic systems are modelled as arrays of infinite cylinders of circular cross section made up of isotropic materials A_i embedded in an infinite isotropic matrix B. The elastic cylinders, of radius R_i, are assumed to be parallel to the x_3-axis of the Cartesian coordinate system $(Ox_1x_2x_3)$ ($\boldsymbol{e}_1, \boldsymbol{e}_2, \boldsymbol{e}_3$ are unit vectors along the x_1-, x_2-, x_3-axis, respectively). The intersections of the cylinder axes with the (x_1Ox_2) transverse plane form a two-dimensional periodic array which resembles the boron nitride crystallographic structure with two kinds of cylinder, A_1 and A_2, in each unit cell. The distance between the nearest neighbours is a (see figure 1). The graphite structure is obtained with cylinders of identical radius and constituted of the same material. The removal of one type of cylinder (A_1 or A_2) from the BN array results in a triangular array of lattice parameter $d = a\sqrt{3}$. The filling fraction f_i of the cylinder A_i, of radius R_i, is defined as the ratio between the cross-sectional area of the rod i and the surface of the unit cell, i.e., for the BN structure,

$$f_i = \frac{\pi R_i^2}{3\sqrt{3}a^2/2}.$$

For the graphite structure ($R_1 = R_2$, i.e. $\alpha = R_1/R_2 = 1$), in the close-packed arrangement ($R_i = a/2$), the maximum value of each f_i is

$$f_i^{\max} = \frac{\pi}{6\sqrt{3}} \cong 0.302.$$

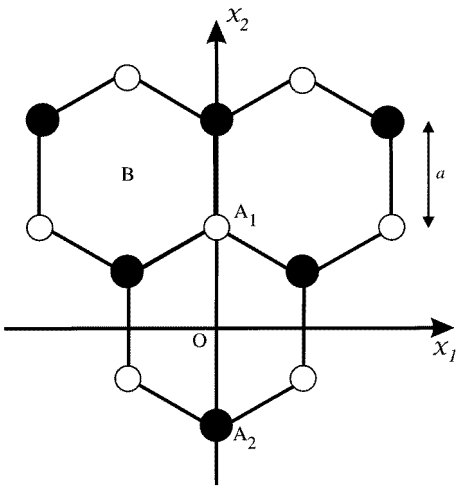

Figure 1. A two-dimensional boron nitride array of infinite cylinders, A_1 (white) and A_2 (black), of different radii, R_1 and R_2, periodically distributed in an infinite matrix B. The cylinders are assumed to be parallel to the x_3-axis perpendicular to the transverse plane (x_1Ox_2), and may be constituted of different materials. The distance between the nearest neighbours is a. The unit cell contains one cylinder of each kind. The graphite structure is obtained for cylinders of identical radius and constituted of the same material. When only one kind of site is occupied, the 2D BN array results in a triangular structure with a lattice parameter $d = a\sqrt{3}$.

In the triangular pattern (with $R_1 = 0$, i.e. $f_1 = 0$ and $\alpha = R_1/R_2 = 0$, for example) the close-packed value of $f_2 = f$ corresponds to $R_2 = d/2$, i.e.

$$f_2^{\max} = f^{\max} = \frac{\pi}{2\sqrt{3}} \cong 0.907.$$

One notices that the maximum filling fraction is lower for the graphite array than for the triangular structure.

We investigate the propagation of elastic waves in the $(x_1 O x_2)$ transverse plane.

With the choice of coordinate axes shown in figure 1, the primitive lattice vectors for the BN structure can be written as

$$\begin{aligned} \boldsymbol{a}_1 &= \frac{a\sqrt{3}}{2}(1, \sqrt{3}) \\ \boldsymbol{a}_2 &= \frac{a\sqrt{3}}{2}(-1, \sqrt{3}). \end{aligned} \tag{1}$$

The two infinite cylinders of the primitive unit cell are located at the positions

$$\boldsymbol{r}_1 = -\boldsymbol{r}_2 = a\sqrt{3}\left(0, \frac{1}{\sqrt{3}}\right). \tag{2}$$

The primitive vectors of the reciprocal lattice are given by

$$\begin{aligned} \boldsymbol{b}_1 &= \frac{2\pi}{a\sqrt{3}}\left(1, \frac{1}{\sqrt{3}}\right) \\ \boldsymbol{b}_2 &= \frac{2\pi}{a\sqrt{3}}\left(-1, \frac{1}{\sqrt{3}}\right) \end{aligned} \tag{3a}$$

and the two-dimensional reciprocal-lattice vectors $\boldsymbol{G}$ are then

$$\boldsymbol{G} = h_1\boldsymbol{b}_1 + h_2\boldsymbol{b}_2 = \frac{2\pi}{a\sqrt{3}}\left[(h_1 - h_2)\boldsymbol{e}_1 + \frac{1}{\sqrt{3}}(h_1 + h_2)\boldsymbol{e}_2\right] \tag{3b}$$

where h_1 and h_2 are two integers.

2.2. The method of calculation

The method of calculation is the well known plane-wave method, where the densities and the elastic constants of the isotropic constituent materials, which are position dependent in the composite system, are developed in 2D Fourier series in the reciprocal space. We summarize here this method for solid/solid and fluid/fluid 2D systems.

Throughout this paper, the matrix and inclusions are constituted of isotropic materials described by linear elasticity. The mass density and the elastic constants are ρ_{A_i}, $C_{11_{A_i}}$, and $C_{44_{A_i}}$ ($i = 1$ or 2) inside the cylinders A_i, and ρ_B, C_{11_B}, and C_{44_B} in the background B. These physical characteristics in the composite system, denoted as ζ in a general way, are space dependent with respect to the position vector $\boldsymbol{r} = (x_1, x_2)$ in the transverse plane, i.e. $\zeta(\boldsymbol{r}) = \zeta_{A_i}$ in the cylinder A_i and $\zeta(\boldsymbol{r}) = \zeta_B$ in the matrix B.

In the 2D solid/solid binary composite material, in the absence of an external force, the equations of motions are

$$\rho(\boldsymbol{r})\frac{\partial^2 u_i}{\partial t^2} = \boldsymbol{\nabla}\cdot[C_{44}(r)\,\boldsymbol{\nabla}u_i] + \boldsymbol{\nabla}\cdot\left[C_{44}(\boldsymbol{r})\frac{\partial \boldsymbol{u}}{\partial x_i}\right] + \frac{\partial}{\partial x_i}[(C_{11}(\boldsymbol{r}) - 2C_{44}(r))\boldsymbol{\nabla}\cdot\boldsymbol{u}] \tag{4}$$

where $\boldsymbol{u}(\boldsymbol{r}, t)$ is the position- and harmonic time-dependent displacement vector, with components u_i ($i = 1, 2, 3$) in the Cartesian coordinate system $(O x_1 x_2 x_3)$. If we limit

the wave propagation to the (x_1Ox_2) transverse plane, one can introduce a 2D wave vector $\boldsymbol{K}(K_1, K_2)$ (which means $K_3 = 0$), and the harmonic displacement vector $\boldsymbol{u}$ is independent of the x_3-coordinate. Then, equation (4) can be separated into the following two equations:

$$\rho(\boldsymbol{r})\frac{\partial^2 u_i}{\partial t^2} = \boldsymbol{\nabla}_T \cdot [C_{44}(r)\,\boldsymbol{\nabla}_T u_i] + \boldsymbol{\nabla}_T \cdot \left[C_{44}(\boldsymbol{r})\frac{\partial \boldsymbol{u}_T}{\partial x_i}\right] + \frac{\partial}{\partial x_i}[(C_{11}(r) - 2C_{44}(\boldsymbol{r}))\boldsymbol{\nabla}_T \cdot \boldsymbol{u}_T] \tag{5}$$

($i = 1$ or 2) with $\boldsymbol{u}_T = u_1\boldsymbol{e}_1 + u_2\boldsymbol{e}_2$ and $\boldsymbol{\nabla}_T = \boldsymbol{e}_1\,\partial/\partial x_1 + \boldsymbol{e}_2\,\partial/\partial x_2$, and

$$\rho(r)\frac{\partial^2 u_3}{\partial t^2} = \boldsymbol{\nabla} \cdot [C_{44}(r)\,\boldsymbol{\nabla} u_3]\,. \tag{6}$$

Equation (6) corresponds to pure transverse modes of vibrations ($u_3\boldsymbol{e}_3 \perp \boldsymbol{K}$) called Z-modes. Equation (5) describes modes of vibrations for which $\boldsymbol{u}_T$ and $\boldsymbol{K}$ are coplanar vectors, which are denoted as XY-modes [8].

In the 2D fluid/fluid binary composite systems, only longitudinal waves ($C_{44} = 0$) are allowed, and the general equation of motion (equation (4)) becomes

$$\rho(r)\frac{\partial^2 \boldsymbol{u}}{\partial t^2} = \boldsymbol{\nabla}(C_{11}(r)\boldsymbol{\nabla} \cdot \boldsymbol{u}). \tag{7}$$

However, the displacement field $\boldsymbol{u}(\boldsymbol{r}, t)$ can be obtained from a scalar potential $\Phi(\boldsymbol{r}, t)$ such that

$$\rho\boldsymbol{u} = \boldsymbol{\nabla}\Phi. \tag{8}$$

Then equation (7) may be rewritten as

$$\left(\frac{1}{C_{11}(\boldsymbol{r})}\right)\frac{\partial^2 \Phi}{\partial t^2} = \boldsymbol{\nabla} \cdot \left(\left(\frac{1}{\rho(\boldsymbol{r})}\right)\boldsymbol{\nabla}\Phi\right). \tag{9}$$

One observes that equation (9) is formally the same as equation (6). Indeed, replacing in equation (9), $1/C_{11}$, $1/\rho$, and Φ by ρ, C_{44}, and u_3 respectively, one obtains equation (6) [2, 13]. We must keep in mind that in fluids, C_{11} stands for the compressibility χ of the material.

In our calculations of elastic band structure of 2D binary composite systems, equations (5), (6), and (9) are the basic equations. Taking advantage of the 2D periodicity in the (x_1Ox_2) plane, the quantities $\rho(\boldsymbol{r})$, $C_{11}(\boldsymbol{r})$, and $C_{44}(\boldsymbol{r})$ for solid/solid composites and $1/\rho(\boldsymbol{r})$, and $1/C_{11}(\boldsymbol{r})$ for fluid/fluid inhomogeneous media are developed in Fourier series in the form

$$\zeta(\boldsymbol{r}) = \sum_{\boldsymbol{G}} \zeta(\boldsymbol{G})\mathrm{e}^{\mathrm{i}\boldsymbol{G}\cdot\boldsymbol{r}}. \tag{10}$$

The Fourier coefficients in equation (10) are given as

$$\zeta(\boldsymbol{G}) = \zeta_{\mathrm{B}}\delta_{\boldsymbol{G}\boldsymbol{0}} + \sum_i \zeta_{\mathrm{A}_i}(\boldsymbol{G})\mathrm{e}^{-\mathrm{i}\boldsymbol{G}\cdot\boldsymbol{r}_i} \tag{11}$$

where the $\boldsymbol{r_i}$ ($i = 1, 2$) are defined in equation (2), δ is the Kronecker symbol, and

$$\zeta_{\mathrm{A}_i}(\boldsymbol{G}) = (\zeta_{\mathrm{A}_i} - \zeta_{\mathrm{B}})F_i(\boldsymbol{G}). \tag{12}$$

In equation (12), $F_i(\boldsymbol{G})$ stands for the structure factor [8–10] of the cylinder i defined as

$$F_i(\boldsymbol{G}) = 2f_i\frac{J_1(GR_i)}{GR_i} \tag{13}$$

where $J_1(x)$ is the Bessel function of the first kind of order one.

The method of calculation for BN structures is strictly equivalent to the one used for square [8–10] and triangular arrays [12, 13]. After some algebra, equations (5), (6), and (9) become standard eigenvalue equations for which the size of the matrices involved depends on the number of $\boldsymbol{G}$-vectors taken into account in the Fourier series.

3. Numerical results for the BN structure

We present, in this section, band structures calculated for 2D binary fluid/fluid and solid/solid composite systems with BN structure. For solid inhomogeneous media, the constituent materials are carbon or tungsten for the inclusions (or the matrix) and epoxy for the matrix (or the inclusions), while for the fluid/fluid systems, water and mercury are the two components. The choice of these materials is based on the strong contrast in their densities and elastic properties, which are listed in tables 1 and 2. We shall compare our results on the BN structure with those obtained previously for square lattices of C cylinders in an epoxy matrix [8] and triangular arrays of water (or mercury) rods in mercury (or water) background [13]. Let us recall that according to the ratio between the radii of the two cylinders in the unit cell, $\alpha = R_1/R_2$, the BN structure takes into account both the triangular pattern and the graphite structure. Indeed, for $\alpha = 0$, one obtains a triangular array of lattice parameter $a\sqrt{3}$, while for $\alpha = 1$, the two cylinders being constituted of the same material, the graphite structure is created. The effect of the parameter α and the influence of the total filling fraction $f = f_1 + f_2$ on the band structure are investigated intensively in this paper.

Table 1. The densities and elastic constants of carbon [22], tungsten [23], and epoxy resin [22]. C_l and C_t represent the longitudinal and the transverse velocities of sound, respectively.

	ρ (g cm^{-3})	C_l (m s^{-1})	C_t (m s^{-1})	$C_{11} = \rho C_l^2$ (10^{10} N m^{-2})	$C_{44} = \rho C_t^2$ (10^{10} N m^{-2})
Carbon	1.75	13 310	7110	30.96	8.846
Tungsten	19.3	5090	2800	50.1	15.14
Epoxy	1.2	2830	1160	0.964	0.161

Table 2. Densities and longitudinal elastic constants for sea-water (at 25 °C) and mercury [24]. C_l represents the longitudinal velocity of sound.

	ρ (g cm^{-3})	C_l (m s^{-1})	$C_{11} = \rho C_l^2$ (10^{10} N m^{-2})
Water	1.025	1531	0.24
Mercury	13.5	1450	2.84

3.1. 2D fluid/fluid binary composite systems

We solved the Fourier transform of equation (9) numerically for the longitudinal modes of vibrations in 2D fluid/fluid binary composite systems. In these calculations, we took into account the 169 shortest $\boldsymbol{G}$-vectors. These vectors are generated in such a way that they are inscribed in a disk of a certain radius. This number of $\boldsymbol{G}$-vectors ensures sufficient

convergence, and offers a good compromise between accuracy and computing time. We consider the case of water (or mercury) cylinders in a mercury (or water) background. As suggested by Kushwaha and Halevi [13], one can imagine that, in practice, the liquid within the cylinders would be contained by some latex material. The mass density and speed of sound in rubber are comparable to those of water, and the effect of this thin latex partition can be neglected. Moreover, these authors have found that for $f = 0.27$, the triangular band structure of water cylinders in a mercury background exhibits the widest gaps ever reported in the literature. In the opposite situation, i.e. a triangular pattern of mercury cylinders in a water background, they have shown the existence of band gaps for $0.45 < f < 0.825$, the maximal width of the lowest stop-band being obtained for $f = 0.75$ (see figure 2 of reference [13]). Thus, in order to compare our results with those published by these authors, we have calculated the dispersion curves of BN arrays of water/mercury systems for $f = f_1 + f_2 = 0.27$ and 0.6, and investigated the evolution of the width of the gaps versus the parameter $\alpha = R_1/R_2$. Let us note that the close-packed configuration of the graphite structure is obtained for $f = f_1 + f_2 \cong 0.604$. These dispersion curves have been plotted for the first ten bands in the principal symmetry directions of the first Brillouin zone (see figure 2).

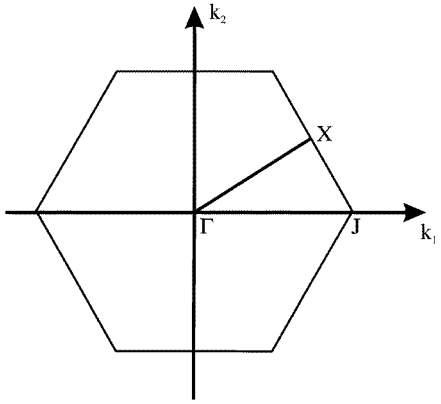

Figure 2. The first Brillouin zone of the BN array. The irreducible part of this regular hexagon is the triangle ΓJX, where the reduced coordinates ($\boldsymbol{k} = \boldsymbol{K}a\sqrt{3}/(2\pi)$, $\boldsymbol{K}$ being a two-dimensional wave vector) of the symmetry points Γ, J, and X in the (x_1Ox_2) plane are respectively $(0, 0)$, $(2/3, 0)$, and $(1/2, 1/2\sqrt{3})$.

Figure 3(a) shows the band structure for the BN array of water cylinders in a mercury background with $f_1 + f_2 = 0.27$ and $\alpha = R_1/R_2 = 0.5345$. The plots are given in terms of the reduced frequency $\Omega = \omega a\sqrt{3}/(2\pi\overline{C_l})$ (with $\overline{C_l} = \sqrt{\overline{(1/\rho)}/\overline{(1/C_{11})}}$ where $\overline{(1/\rho)} = (1/\rho)(\boldsymbol{G} = \boldsymbol{0})$ and $\overline{(1/C_{11})} = (1/C_{11})(\boldsymbol{G} = \boldsymbol{0})$ (see equation (11))) versus the reduced Bloch wave vector $\boldsymbol{k} = \boldsymbol{K}a\sqrt{3}/(2\pi)$. There exist five acoustic band gaps in the frequency domain of figure 3(a), the largest appearing between the second and the third band with $\Delta\Omega \approx 0.37$. Figure 3(b) shows the dependence of these gaps versus the parameter α for $f_1 + f_2 = 0.27$. For α varying between 0 and 1, the BN array evolves from triangular to graphite structure. In the range of frequency $0 < \Omega < 2$, one very large gap appears in the band structure of the triangular pattern ($\alpha = 0$) for $0.27 < \Omega < 0.82$, i.e. $\Delta\Omega = 0.55$. This stop-band corresponds to the widest gap obtained by Kushwaha and Halevi (see figure 2 of reference [13]). The width of this gap decreases with increasing α, and reaches its

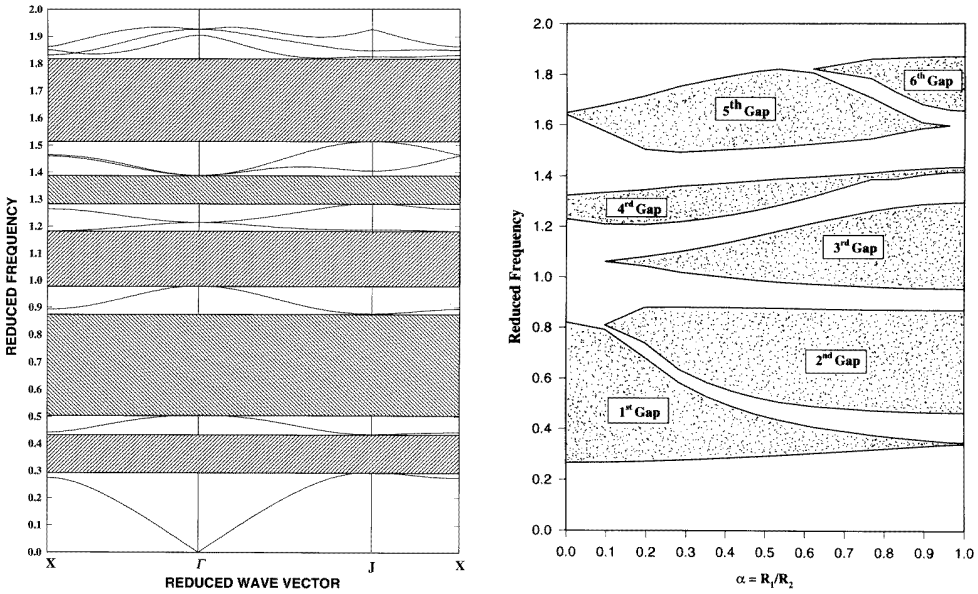

(a) (b)

Figure 3. (a) The elastic band structure for the BN array of water cylinders in a mercury background for $f_1 + f_2 = 0.27$ and $\alpha = R_1/R_2 = 0.5345$ (f_i and $R_i, i = 1$ or 2, are respectively the filling fraction and the radius of the two cylinders in the unit cell). The band structure is plotted for the longitudinal modes of vibration in the three high-symmetry directions ΓJX of the first Brillouin zone (see figure 2). One can notice five gaps in the range of frequency $0 < \Omega < 1.9$. (b) The variation of the width of the gaps appearing in the band structure of the BN array of water cylinders in a mercury background, for $f_1 + f_2 = 0.27$, as a function of the parameter $\alpha = R_1/R_2$.

minimum value for the graphite structure ($\alpha = 1$). An interesting result is the existence of three additional gaps (the second, third, and sixth gaps appearing with increasing Ω) in the band structure of the BN pattern for $0.1 < \alpha < 1$. The width of these gaps increases with increasing α and is maximal in the graphite structure. One observes also that the width of the fifth gap is maximal for $\alpha \cong 0.5$. Compared to the triangular pattern ($\alpha = 0$), the BN structure of this 2D binary fluid/fluid composite system presents some large additional gaps in the same range of frequency. The narrowness of the pass-bands is also remarkable in this composite. The BN band structures for this 2D binary composite were also calculated for $f_1 + f_2 = 0.6$, and lead to qualitatively similar conclusions, although the gaps are narrower in this case. In particular, the largest gap found in the triangular band structure has a width $\Delta\Omega$ equal to 0.42.

We have also considered the opposite situation, i.e. the BN array of mercury cylinders in a water background. Figure 4(a) shows the band structure in this case for $f_1 + f_2 = 0.6$ and $\alpha = 0.642$. There exist three gaps in figure 4(a), the largest appearing between the first and the second band with $\Delta\Omega \approx 0.368$. Figure 4(b) shows the width of the gaps versus the parameter α for $f_1 + f_2 = 0.60$ in the range of frequency $0 < \Omega < 2$. For $\alpha = 0$, the second gap, centred on $\Omega = 1$ with a width $\Delta\Omega \cong 0.1$, corresponds to the one observed by Kushwaha and Halevi (see figure 2 of reference [13]) in the triangular lattice. One observes that the third gap (with increasing Ω) exists only in the BN structure for $0.25 < \alpha < 0.9$, and reaches its maximal width around $\alpha \cong 0.65$. The largest gap is obtained for $\alpha = 1$

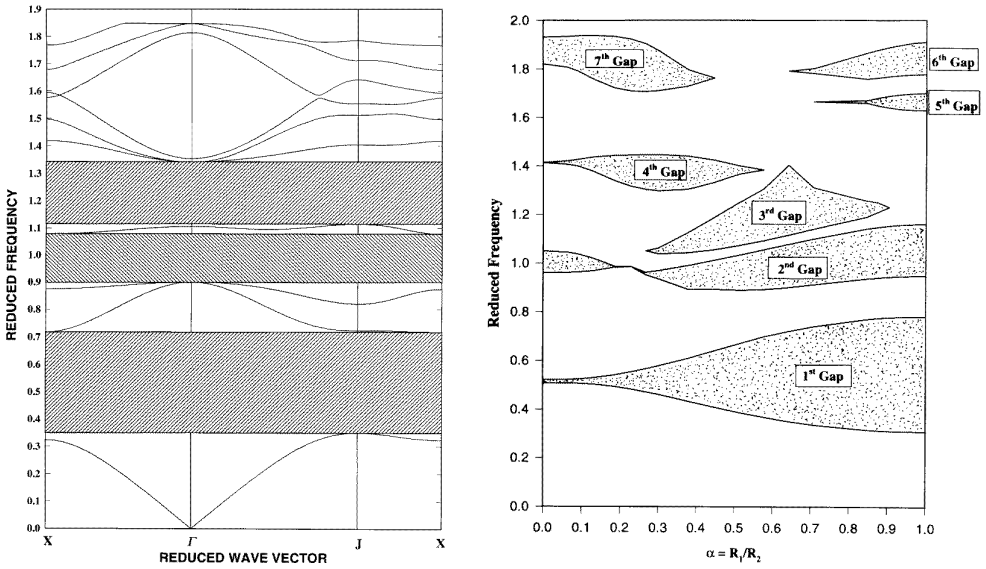

(a) (b)

Figure 4. (a) The elastic band structure for the BN array of mercury cylinders in a water background for $f_1 + f_2 = 0.60$ and $\alpha = R_1/R_2 = 0.642$. One can notice three gaps in the range of frequency $0 < \Omega < 1.9$. (b) The variation of the widths of the gaps appearing in the band structure of the BN array of mercury cylinders in a water background, for $f_1 + f_2 = 0.60$, as a function of the parameter $\alpha = R_1/R_2$.

between the first and the second band (see figure 4(a)). For $f_1 + f_2 = 0.6$, the graphite structure ($\alpha = 1$) is very near to the close-packed configuration for which $f_1 + f_2 \cong 0.604$, and where each cylinder is in contact with another. The technical realization of this structure would probably be very difficult, because the background material separating two cylinders becomes very thin. However, the contact between cylinders can be avoided by using the BN geometry with α quite different from 1, even for this maximum filling fraction. These results reveal that for mercury cylinders in a water background, the general BN structure, and in particular the graphite pattern, is more favourable for the opening of large gaps in the band structure while the triangular structure is less appropriate. Moreover, for high filling fractions, the choice of cylindrical inclusions of different diameters allows an easier technical manufacturing process together with the possibility of keeping large absolute band gaps.

It is noteworthy that for $f_1 + f_2 = 0.6$, the graphite band structure of mercury cylinders in a water background presents some similarities with the triangular band structure of circular water rods in a mercury matrix, especially for the dispersion of the low-frequency bands. Following the observations of Cassagne *et al* [19] on photonic crystals, this can be understood from the disposition of the cylinders in the graphite structure. From a geometric point of view, in the close-packed arrangement, the graphite array of mercury cylinders in a water background is equivalent to a triangular structure of lattice parameter $a\sqrt{3}$ constituted of water rods with non-circular cross section embedded in a mercury matrix.

In order to investigate the effect of the filling fraction on the band structure, we have also calculated the dispersion curves for the BN array of mercury cylinders in a water background for $f_1 + f_2 = 0.30$. There is no gap in the triangular band structure, while

the graphite pattern gives rise to a single gap between the first and the second band with $\Delta\Omega \approx 0.142$. One can notice that the density of mercury is greater than that of the water, while the speeds of sound in these materials are nearly the same. One can assume that, for any value of the total filling fraction, in 2D binary fluid/fluid composite systems, the largest acoustic band gaps appear for triangular structure of low-density inclusions in a high-density background or for a graphite array of high-density rods in a low-density matrix. This result parallels those of Cassagne *et al* [19] for photonic crystals. These authors have shown that the largest photonic absolute band gaps appear for triangular structure of cylindrical holes in a dielectric or for graphite structures of dielectric rods in air. This is easily understandable by considering the analogy between the Maxwell equations and linear elasticity in fluids. For α quite different from 0 and 1, the BN array gives rise to additional large gaps in the same range of frequency.

3.2. 2D solid/solid binary composite systems

In a previous work [8], we have shown that the acoustic band structure of a square array of carbon fibres embedded in an epoxy matrix exhibits large absolute band gaps; the widest gaps are obtained for a filling fraction $f = 0.55$ (see figure 2(b) of reference [8]). In complement to this work, we have calculated the dispersion curves for triangular arrays of carbon rods in an epoxy background, considering various filling fractions. With this pattern, the widest gap was obtained for $f = 0.65$. Its width is 1.7 times larger than the one obtained for the square array [8]. In this case, the triangular structure is more favourable than the square pattern for the opening of absolute gaps in the acoustic band structure of 2D binary solid/solid composite material. This observation is in agreement with previous results obtained independently by Sigalas and Economou [11] and Kushwaha and Halevi [12] for other constituents of the 2D inhomogeneous material.

In this section, we extend our investigation to 2D composite materials of BN structure, the constituent materials being C (or W) and epoxy. Both cases of high and low filling fractions of the inclusions will be considered; that is, we shall assume either $f_1 + f_2 = 0.6$ (which is the nearest value to 0.65 available for the BN structure) or $f_1 + f_2 = 0.3$, and discuss the behaviour of the acoustic band gaps versus the parameter $\alpha = R_1/R_2$.

The calculation is performed by solving numerically the Fourier transforms of equations (5) and (6) for the XY- and Z-modes of vibrations, taking into account the 169 shortest $\boldsymbol{G}$-vectors. The plots are given in terms of the reduced frequency $\Omega = \omega a\sqrt{3}/(2\pi C_0)$ (with $C_0 = \sqrt{\bar{C}_{44}/\bar{\rho}}$ where $\overline{C_{44}} = C_{44}(G = 0)$ and $\bar{\rho} = \rho(\boldsymbol{G} = \boldsymbol{0})$ (see equation (11))) versus the reduced Bloch wave vector $\boldsymbol{k} = \boldsymbol{K}a\sqrt{3}/(2\pi)$.

Let us first consider the filling fraction $f_1 + f_2 = 0.6$. Figure 5(a) presents the first ten acoustic Z- and XY-bands when the ratio between the radii of the two cylinders in the BN structure is given by $\alpha = 0.186$. One can observe that there are five complete band gaps in this band structure, the largest appearing between the third XY-band and the second Z-band with $\Delta\Omega \approx 0.048$. The presence of nearly flat bands such as the second or the fourth Z-bands may indicate the existence of localized states in this structure. The effect of the parameter α on the band structure is investigated in figure 5(b) where we have superimposed the variations of the width of the Z- (dashed lines) and XY- (solid lines) band gaps versus the parameter α for $f_1 + f_2 = 0.6$. Numerous wide Z-gaps appear for $0 < \alpha < 0.5$. The existence of a large XY-gap, between the third and the fourth XY-bands (see figure 5(a)), for $0.33 < \Omega < 0.57$, gives rise to three absolute band gaps where the propagation of acoustic waves of any polarization is forbidden. These absolute gaps are represented as speckled areas in figure 5(b). One can notice that the second absolute band

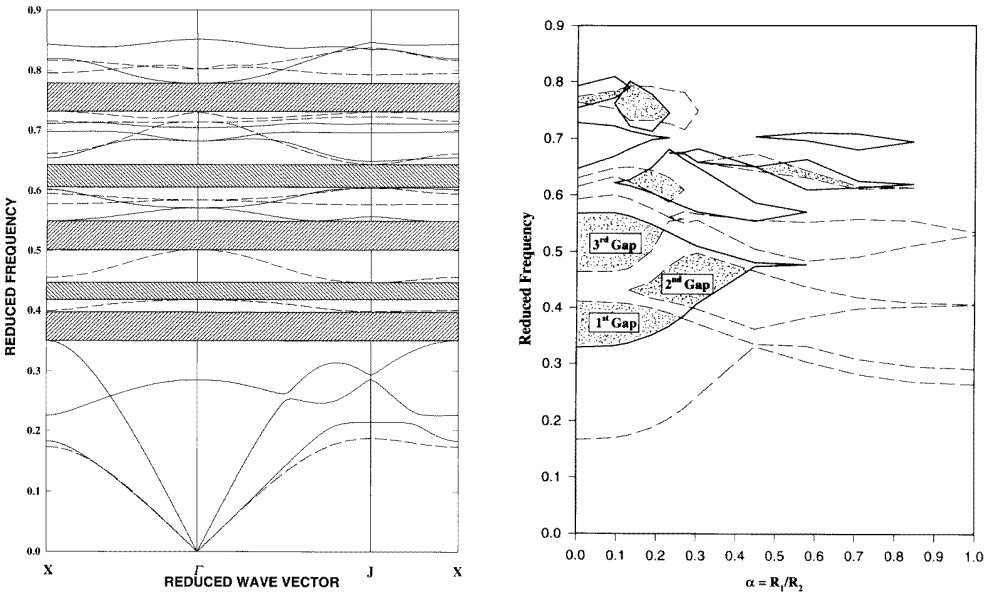

(a) (b)

Figure 5. (a) The elastic band structure for a BN array of C cylinders in an epoxy resin matrix for $f_1 + f_2 = 0.6$ and $\alpha = R_1/R_2 = 0.186$. The band structure is plotted for Z- (dashed lines) and XY- (solid lines) modes of vibration in the three high-symmetry directions ΓJX of the first Brillouin zone (see figure 2). One can notice five complete band gaps in the range of frequency $0 < \Omega < 0.9$. (b) The variation of the width of the Z- (dashed lines) and XY- (solid lines) gaps appearing in the band structure of the BN arrays of carbon cylinders in an epoxy background, for $f_1 + f_2 = 0.60$, as a function of the parameter $\alpha = R_1/R_2$. Each pair of dashed lines (or solid lines) represents the variation of the lower and upper frequencies for each Z- (or XY-) gap as a function of α. The overlap of the Z- and XY-gaps results in absolute band gaps represented as speckled areas in this figure.

gap which opens for $0.4 < \Omega < 0.5$ exists only in the BN structure with $0.13 < \alpha < 0.45$. The maximum width of this gap, obtained for $\alpha \approx 0.3$, is of the same order of magnitude as the largest gap observed in the triangular structure. One can imagine for this kind of composite material engineering applications such as very selective acoustic filters. There is no absolute band gap in the graphite band structure, i.e. for $\alpha = 1$. This result shows that the contrast between the diameters of the two cylinders plays an important role in determining acoustic band gaps.

We have also investigated the inverse situation, i.e. the BN array of epoxy cylinders in a carbon background for $f_1 + f_2 = 0.6$. As can be observed in figure 6, absolute band gaps appear in this band structure for $0.4 < \alpha < 1$. The largest absolute gap, centred on $\Omega = 0.45$, is obtained in the graphite structure with $\Delta\Omega \cong 0.07$. For small α, most of the Z- and XY-gaps are very narrow except the first Z-gap. For α close to 1, there exist some large Z-gaps. It is noticeable that in the case of square arrays of epoxy cylinders in a carbon matrix, the band structure does not present absolute band gaps [8]. We deduce that, for such a high filling fraction, the existence of band gaps is more favoured in triangular arrays of inclusions having a density and elastic constants greater than those of the matrix. If the background is the component of greater density and elastic constants, the graphite structure is more appropriate.

Similar studies were performed for BN arrays of W (or epoxy) cylinders in an epoxy (or W) background for $f_1 + f_2 = 0.6$. Large absolute band gaps were obtained for BN arrays of W cylinders in an epoxy background with $0 < \alpha < 0.65$ as well as for BN arrays of epoxy cylinders in a W background with $0.30 < \alpha < 1$, the largest gaps being observed for the triangular structure in the first case and for the graphite geometry in the second case. The absolute band gaps in composite materials made of W and epoxy are larger than those observed in C–epoxy BN structures. This result can be explained by the contrast between the densities of W and C (see table 1).

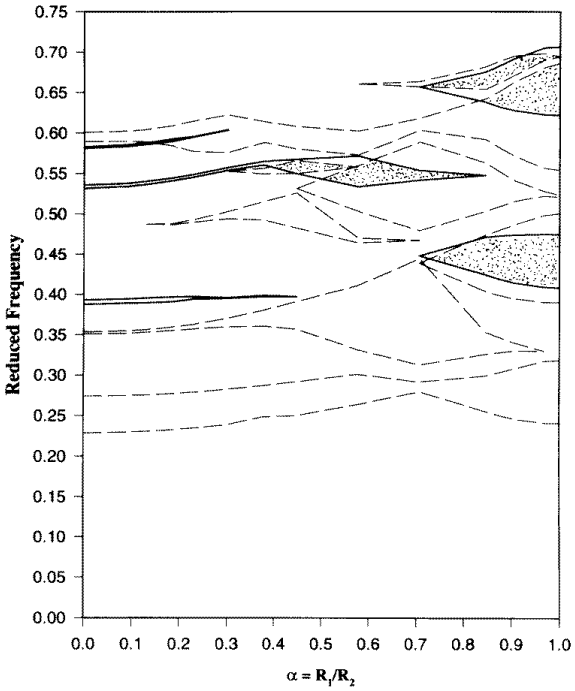

Figure 6. The variation of the width of the Z- (dashed lines) and XY- (solid lines) gaps appearing in the band structure of the BN arrays of epoxy cylinders in a carbon background, for $f_1 + f_2 = 0.60$, as a function of the parameter $\alpha = R_1/R_2$. The absolute band gaps are represented as speckled areas in this figure.

It is noteworthy that for this filling fraction, $f_1 + f_2 = 0.6$, the first few dispersion curves in the graphite band structure of the epoxy/C (or W) system show some similarities with the corresponding curves in the triangular band structure of the C (or W)/epoxy composite. A similar observation was made in section 3.1 for 2D binary fluid/fluid composites in relation to the results obtained for photonic crystals [18, 19] . Finally, we would emphasize that at such a high filling fraction near to the close-packed arrangement in the graphite structure, the BN geometry offers the possibility of avoiding contact between the cylinders together with the existence of large absolute band gaps.

We now come to consider the case of a low filling fraction such as $f_1 + f_2 = 0.3$. In this case, there are no absolute band gaps in the BN arrays of epoxy fibres in a C or W background. Absolute gaps were obtained for composites made up of C or W fibres in epoxy, the widths of these gaps being much larger for W fibres than with C inclusions. Figure 7(a) shows the first acoustic Z- and XY-bands, in the range of frequency

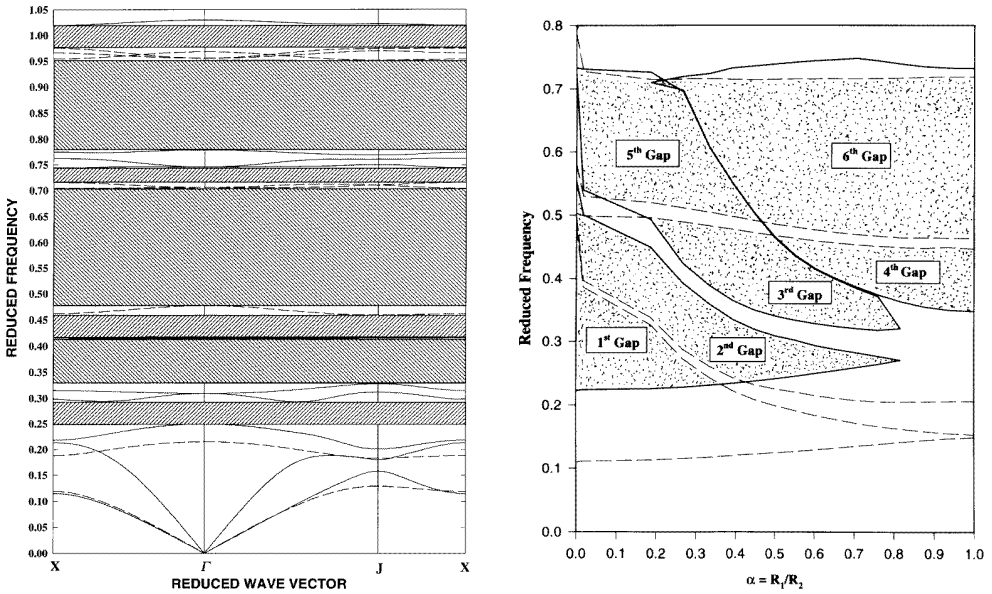

(a) (b)

Figure 7. (a) The elastic band structure for a BN array of tungsten cylinders in an epoxy resin matrix for $f_1 + f_2 = 0.3$ and $\alpha = R_1/R_2 = 0.603$. The band structure is plotted with the same conventions as in figure 5(a). One can notice seven complete band gaps in the range of frequency $0 < \Omega < 1.05$. (b) The variation of the width of the Z- (dashed lines) and XY- (solid lines) gaps appearing in the band structure of the BN array of tungsten cylinders in an epoxy background, for $f_1 + f_2 = 0.30$, as a function of the parameter $\alpha = R_1/R_2$ for $0 < \Omega < 0.8$. The absolute band gaps are represented as speckled areas.

$0 < \Omega < 1.05$, for the BN array of W cylinders in an epoxy matrix with $f_1 + f_2 = 0.30$ and $\alpha = R_1/R_2 = 0.603$. There are seven absolute gaps in this band structure; the largest appears between the third and the fourth Z-bands with $\Delta\Omega = 0.228$. Most of the Z- and XY-bands, especially those at high frequencies, are very flat. The fourth and the fifth absolute gaps are very much larger than those obtained in figure 5(a). In figure 7(b), we present the dependence of the Z- and XY-gaps in the band structure of W/epoxy BN arrays versus the parameter $\alpha = R_1/R_2$ for $0 < \Omega < 0.8$. The width of the first absolute band gap is maximal for $\alpha = 0$, strongly decreases for α slightly different from zero, and then reaches its minimum value for $\alpha \cong 0.8$. One observes that a very large Z-gap exists for all values of α, for $0.5 < \Omega < 0.7$. This gap appears between the third and the fourth Z-bands in the band structure (see figure 7(a)), and the maximum of its width occurs for $\alpha = 1$. For $0.25 < \alpha < 0.75$ and $0.4 < \Omega < 0.7$, the upper limit of the second XY-gap and the lower limit of the third XY-gap merge together. These two gaps are delimited by the sixth XY-band (see figure 7(a)) which is strictly flat for these values of α and Ω. The first and the sixth absolute band gaps (of maximum width for $\alpha = 1$) have widths of the same order of magnitude ($\Delta\Omega = 0.26$ for the first and $\Delta\Omega = 0.244$ for the sixth). One observes also that the third absolute band gap which opens for $0.35 < \Omega < 0.5$ exists only in the BN structure with $0.15 < \alpha < 0.80$, and reaches its maximum width for $\alpha \approx 0.5$. For $f_1 + f_2 = 0.3$, the BN array of W cylinders in an epoxy matrix is a good candidate for the opening of absolute band gaps with a configuration far from the close-packed arrangement.

4. Conclusions

The purpose of this paper was to investigate the existence of absolute band gaps in the acoustic band structure of a new class of two-dimensional binary periodic composite systems: the boron nitride array of infinite parallel cylinders in a background. In this pattern, the unit cell contains two cylinders of different diameters, and the rods are located at the vertices of a regular hexagon. We have considered artificial materials for which the inclusions and matrix are either both solids or both fluids, such as carbon or tungsten (or epoxy) fibres in an epoxy (or C or W) matrix, or water cylinders (or mercury) in a mercury (or water) background.

We obtained relatively large complete gaps where the propagation, perpendicular to the inclusions, of phonons in the acoustic region is forbidden. These gaps are larger for fluid/fluid than for solid/solid binary composites. This result can be understood on the basis that fluids can only support longitudinal modes of vibration. The influence of the cylinder diameters as well as the effect of the composition of the composite material on the band structure were studied.

For high filling fractions, the triangular structure of C or W cylinders embedded in an infinite epoxy matrix is more favourable for the opening of very large gaps in the band structure. In the opposite situation, i.e. epoxy fibres in a C or W background, the graphite structure, in which all the cylindrical inclusions have the same radius, is more appropriate. For quite low filling fractions, triangular and graphite arrays of W cylinders in an epoxy matrix give rise to large absolute acoustic band gaps of qualitatively similar width. Our results demonstrate also that 2D solid/solid BN structures with cylinders of markedly different radii may be used as selective frequency filters.

For 2D binary fluid/fluid composites, the graphite structure yielded the largest acoustic band gaps when cylinders of a high-density material were embedded in a background of low density; this is the case independently of the filling fraction of the inclusions. In the opposite case of low-density fibres embedded in a high-density matrix, the triangular structure gives rise to one large absolute band gap (which is the largest one that we have obtained), but in graphite and some BN geometries one can obtain several gaps having qualitatively the same order of magnitude. Moreover in the limit of a high filling fraction, the BN geometry offers the possibility of an easy technical realization which avoids the contact between the fibres.

In solid composites, one may of course be interested in a separate study (or experimental excitation) of Z- and XY-polarized modes. In this respect, it is worthwhile to notice the similarities between the wave equation which describes the Z-polarized modes in solid composites and the one giving the fluid composite band structure. This comparison can be made by replacing the parameters ρ and C_{44} in a solid respectively by $1/C_{11}$ and $1/\rho$ in the fluid. Then the conclusions mentioned above for fluid composites can also explain or predict the behaviours of the band structure for Z-polarized modes in solid composites. For instance, in the case of epoxy fibres in a C (or W) matrix (which means $C_{44_A} \ll C_{44_B}$ and $\rho_A \ll \rho_B$) the largest Z-polarized gaps were obtained in the graphite and some BN geometries. In the opposite case of C (or W) cylinders in an epoxy matrix, the triangular structure gave the largest gap, although the BN patterns with $\alpha \neq 0$, and in particular the graphite structure, show richer band-gap structures.

Our calculation of the acoustic band structure was performed in this work for waves propagating parallel to the (x_1Ox_2) plane (perpendicular to the x_3-axis of the fibres). For infinitely long cylinders, it is likely that these gaps will close if we take account of wave propagation along the x_3-direction in addition to the propagation along the x_1- and x_2-

directions. However, one may assume that these gaps will still exist either if the cylinders are of finite dimension with a length of order π/a, or if they are composed of a periodic structure with a repeating period of the same order of magnitude [21].

Finally, it could be interesting to extend our calculation to two-dimensional mixed periodic composite media where the inclusions and matrix are of different nature, i.e. fluid (or solid) cylinders, disposed on patterns of various geometries, in a solid (or fluid) matrix. The experimental manufacturing of these systems will of course be very easy.

Acknowledgment

This work was partially supported by Le Conseil Régional Nord-Pas de Calais.

References

[1] See, for example,
1994 *J. Mod. Opt.* **41** special issue
and the review article
Pendry J B 1996 *J. Phys.: Condens. Matter* **8** 1085
[2] See the review paper
Kushwaha M S 1996 *Int. J. Mod. Phys.* B **10** 977
[3] Kafesaki M, Sigalas M M and Economou E N 1995 *Solid State Commun.* **96** 285
[4] Kafesaki M, Sigalas M M and Economou E N 1996 *Photonic Band Gap Materials (NATO ASI Series E: Applied Sciences, vol 315)* ed C M Soukoulis (Dordrecht: Kluwer) p 143
[5] Sigalas M and Economou E N 1993 *Localization and Propagation of Classical Waves in Random and Periodic Structures* ed C M Soukoulis (New York: Plenum)
[6] Kushwaha M S and Djafari-Rouhani B 1996 *J. Appl. Phys.* **80** 3191
[7] Sigalas M and Economou E N 1993 *Solid State Commun.* **86** 141
[8] Vasseur J O, Djafari-Rouhani B, Dobrzynski L, Kushwaha M S and Halevi P 1994 *J. Phys.: Condens. Matter* **6** 8759
[9] Kushwaha M S, Halevi P, Dobrzynski L and Djafari-Rouhani B 1993 *Phys. Rev. Lett.* **71** 2022
[10] Kushwaha M S, Halevi P, Martinez-Montes G, Dobrzynski L and Djafari-Rouhani B 1994 *Phys. Rev.* B **49** 2313
[11] Sigalas M M and Economou E N 1993 *J. Appl. Phys.* **75** 2845
[12] Kushwaha M S and Halevi P 1994 *Appl. Phys. Lett.* **64** 1085
[13] Kushwaha M S and Halevi P 1996 *Appl. Phys. Lett.* **69** 31
[14] Dobrzynski L, Djafari-Rouhani B and Hardouin-Duparc O 1984 *Phys. Rev.* B **29** 3138
[15] Camley R E, Djafari-Rouhani B, Dobrzynski L and Maradudin A A 1983 *Phys. Rev.* B **27** 7318
[16] Dowling J P 1992 *J. Acoust. Soc. Am.* **91** 2539
[17] Esquivel-Sirvent R and Cocoletzi G H 1994 *J. Acoust. Soc. Am.* **95** 86
[18] Cassagne D, Jouanin C and Bertho D 1995 *Phys. Rev.* B **52** R2217
[19] Cassagne D, Jouanin C and Bertho D 1996 *Phys. Rev.* B **53** 7134
[20] Plihal M and Maradudin A A 1991 *Phys. Rev.* B **44** 8565
[21] Hornreich R M, Kugler M, Shtrikman S and Sommers C 1997 *J. Physique* I **7** 509
[22] Gay D 1991 *Matériaux Composites* (Paris: Hermès)
[23] *American Institute of Physics Handbook* 1972 3rd edn (New York: AIP)
[24] *CRC Handbook of Chemistry and Physics* 1985 66th edn, ed R C Weast (Boca Raton, FL: Chemical Rubber Company Press)